The effect of the spin-orbit interaction on the electronic structure of magnetic materials

1991 J. Phys.: Condens. Matter 3 5131

(http://iopscience.iop.org/0953-8984/3/27/006)

J. Phys.: Condens. Matter 3 (1991) 5131–5141. Printed in the UK

The effect of the spin–orbit interaction on the electronic structure of magnetic materials

B I Min and Y-R Jang
Department of Physics and Basic Science Research Institute,
Pohang Institute of Science and Technology, Pohang 790-600, Korea

Received 13 September 1990, in final form 7 March 1991

Abstract. In order to investigate the effect of the spin–orbit interaction on strong magnetism, we have developed a method of electronic structure calculation which includes the spin–orbit interaction in an approximate way into the semi-relativistic LMTO Hamiltonian. In this way both the spin–orbit interaction and the magnetic exchange–correlation interaction are taken into account simultaneously in the self-consistent variational step. For a systematic study of the effect of spin–orbit interaction on the electronic structures, we have applied this method to magnetic materials including transition metals such as Fe, Co and Ni and light rare-earth metals from Ce to Gd. Orbital polarizations and the spectroscopic splitting g-factors for these materials are determined and compared with previous theoretical and experimental results.

1. Introduction

For the last decade, extensive studies of the electronic structure of f-electron materials, rare earths and actinides, have been carried out in the framework of self-consistent density functional band-structure calculations. In f-electron materials, it is well known that relativistic effects, especially the spin–orbit interaction, become important owing to their large atomic number. On the other hand, magnetic exchange–correlation interactions are also significant because of the large Coulomb correlation interaction of the f electrons. This fact is revealed in figure 1 which compares the magnitudes of the spin–orbit and the magnetic exchange splittings of 4f-core levels in rare-earth metals [1]. Although the magnetic exchange splittings dominate in elements with a nearly half-filled f shell, the magnitudes of the spin–orbit splittings are also sizeable in the whole series. Therefore both effects should be taken into account properly in describing the band nature of f electrons. A fully relativistic density functional Dirac equation with a periodic potential should be solved. However, one faces an immediate difficulty because spin is not a good quantum number in the relativistic Dirac theory.

Much progress has been made by several groups in developing formalisms for the relativistic extension of the spin-density functional theory [2]. Suggested theories are based on the Hohenberg–Kohn theorem and accordingly the exchange–correlation potential depends not only on the charge density but also on the current density. However, not many practical calculations have been reported because applying this theory to an extended system is very complicated. Quite a few applications have been

0953-8984/91/275131 + 11 $03.50

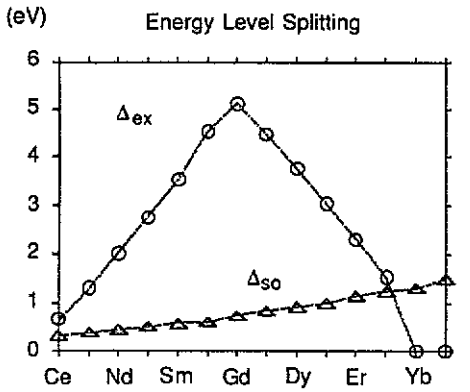

Figure 1. The magnitudes of the exchange–correlation energy splitting Δ_{ex} (○) and the spin–orbit energy splitting Δ_{so} (△) of 4f levels in the rare-earth series.

reported. Among those, Ackermann *et al* [3] applied the effective single-particle Dirac formalism for solids to the band structures of the ferromagnetic Fe and Gd metals but their calculations were not self-consistent and no ground-state properties were studied. More recently, Krutzen and Springelkamp [4] performed self-consistent calculations for ferromagnetic Ni and Gd employing the spin-polarized relativistic augmented-spherical-wave (ASW) band method. Ebert *et al* [5] presented fully relativistic calculational results for the magnetic moments and hyperfine fields of the ferromagnetic Fe, Co and Ni using the multiple-scattering version of the Green function method. Jansen [6] and Daalderop *et al* [7] discussed the crystalline magnetic anisotropy using the relativistic density functional theory.

Conventional electronic band-structure calculations have often employed a semi-relativistic approximation to the fully relativistic Dirac equation which retains the mass–velocity term and Darwin term but not the spin–orbit interaction. It is designed to separate spin-mixing interactions and thus to assume that the spin is still a good quantum number. Therefore approximate pure-spin-basis functions can be used in the same way as in non-relativistic spin-polarized calculations and magnetic exchange–correlation effects can be adequately treated.

In order to describe simultaneously the effects of the spin–orbit interaction and the magnetic exchange–correlation interaction, we attempt in this paper a straightfoward extension of the approximate pure-spin-basis formalism of MacDonald *et al* [8]. We have generalized the semi-relativistic linearized muffin-tin orbital (LMTO) band method to include the spin–orbit interaction, using self-consistent charge densities constructed in the local spin-density approximation. Both semi-relativistic and spin–orbit Hamiltonian matrix elements are constructed simultaneously using the spin basis sets obtained in the self-consistent iterations. The approximation that we have used in this paper is similar to those used by Brooks and Kelly [9], Sticht and Kübler [10], Norman and Koelling [11] and Fritsche *et al* [12]. We use the LMTO band method. Brooks and Kelly also used the LMTO method to calculate the orbital moment contribution to 5f-band magnetism while Sticht and Kübler used the ASW method to determine the electronic structure of Gd. Norman and Koelling used the linearized augmented-plane-wave (LAPW) method to investigate the antiferromagnetic properties of $NpSn_3$, and Fritsche *et al* used the linear rigorous cellular method to calculate the electronic structures of Fe, Ni and Pd. The

main difference of our method is that, for the construction of Hamiltonian matrix elements, we use the spin-dependent radial basis functions which are determined by the self-consistent spin-dependent radial equations, whereas previous methods have used the paramagnetic radial functions. Daalderop *et al* [7] and Eriksson *et al* [13] reported, more recently, self-consistent LMTO band results employing schemes similar to ours. Eriksson *et al* determined the orbital magnetic moments in transition metals Fe, Co and Ni and in an actinide system $NpOs_2$. Daalderop *et al* carried out first-principle calculations of magnetocrystalline anisotropy energies in Fe, Co and Ni.

By means of this procedure, we have investigated the effect of the spin–orbit interaction on the electronic structures of transition metals such as Fe, Co and Ni, and also of the light rare-earth metals Ce to Gd. Orbital contributions to the magnetic moments and the spectroscopic splitting g-factors, both of which originate from the spin–orbit interaction, are determined. In section 2 the computational details that we have used are presented. In section 3, results and discussions are presented and a summary is given in section 4.

2. Computational details

The single-particle Dirac equation to be solved in the solid is

$$H|\Psi_j(\boldsymbol{k})\rangle = [c\boldsymbol{\alpha}\boldsymbol{p} + (\boldsymbol{\beta} - 1)mc^2 + V(\boldsymbol{r})]\,|\Psi_j(\boldsymbol{k})\rangle = \varepsilon_j(\boldsymbol{k})\,|\Psi_j(\boldsymbol{k})\rangle \tag{1}$$

where $\boldsymbol{\alpha}$ and $\boldsymbol{\beta}$ are Dirac matrices and $|\Psi_j(\boldsymbol{k})\rangle$ is a Bloch function which is four-component spinor, and j and $\boldsymbol{k}$ are the band index and the $\boldsymbol{k}$-vector, respectively, inside Brillouin zone. Energy is measured relative to the rest mass energy. Now the Bloch function $|\Psi_j(\boldsymbol{k})\rangle$ is expanded with the LMTO basis $|\Phi(\boldsymbol{k}, L, s)\rangle$:

$$|\Psi_j(\boldsymbol{k})\rangle = \sum_{LS} C_j(\boldsymbol{k}, L, s)\,|\Phi(\boldsymbol{k}, L, s)\rangle \tag{2}$$

where

$$|\Phi(\boldsymbol{k}, L, s)\rangle = \sum_{L'} [|\varphi(L', s)\rangle\, \boldsymbol{\Pi}_{L'L}(\boldsymbol{k}, s) + |\dot{\varphi}(L', s)\rangle\, \boldsymbol{\Omega}_{L'L}(\boldsymbol{k}, s)]. \tag{3}$$

Here $L \equiv (l, m)$ stands for angular momentum and magnetic quantum numbers and s for a spin index. $\boldsymbol{\Pi}$ and $\boldsymbol{\Omega}$ are matrices which are determined for a given $\boldsymbol{k}$-vector by the crystal structure and the boundary condition at the atomic sphere. $|\varphi(L, s)\rangle$ and its energy derivative $|\dot{\varphi}(L, s)\rangle$ are given by the solutions $P_{ls}(r)$, $Q_{ls}(r)$ of the j-weighted semi-relativistic radial Dirac equation and their energy derivatives with a spherical potential $V_s(r)$ inside the atomic sphere [14]. Note that the spin and orbital wavefunctions are separated in $|\varphi(L, s)\rangle$ and $|\dot{\varphi}(L, s)\rangle$.

Following MacDonald *et al* [8], it is easily verified that $|\varphi(L, s)\rangle$ and $|\dot{\varphi}(L, s)\rangle$ satisfy the following equations if the terms of order up to $1/c^2$ are retained:

$$H_a|\varphi(L, s)\rangle = \varepsilon_{ls}\,|\varphi(L, s)\rangle + H^0_{so}|\dot{\varphi}(L, s)\rangle \tag{4}$$

$$H_a|\dot{\varphi}(L, s)\rangle = \varepsilon_{ls}\,|\dot{\varphi}(L, s)\rangle + |\varphi(L, s)\rangle + H^1_{so}|\dot{\varphi}(L, s)\rangle \tag{5}$$

where

$$H_{so}^{0}|\varphi(L,s)\rangle \equiv [1/2M_{ls}^{2}(r)c^{2}](1/r)[\mathrm{d}V_{s}(r)/\mathrm{d}r][P_{ls}(r)/r]\begin{bmatrix} L\cdot SY_{lm}\chi_{s} \\ 0 \end{bmatrix} \tag{6}$$

$$H_{so}^{1}|\dot{\varphi}(L,s)\rangle \equiv [1/2M_{ls}^{2}(r)c^{2}](1/r)[\mathrm{d}V_{s}(r)/\mathrm{d}r][\dot{P}_{ls}(r)/r]\begin{bmatrix} L\cdot SY_{lm}\chi_{s} \\ 0 \end{bmatrix} \tag{7}$$

and

$$M_{ls}(r) = m + (1/2c^{2})[\varepsilon_{ls} - V_{s}(r)]. \tag{8}$$

Here H_{a} denotes a Hamiltonian inside the atomic sphere and H_{so} a spin–orbit interaction operator. ε_{ls} is the energy parameter employed in the linearized band methods and χ_{s} is a two-component spinor.

With the LMTO basis $|\Phi(k, L, s)\rangle$, the standard secular equation of the form

$$\mathbf{HC} = \varepsilon\mathbf{SC} \tag{9}$$

is obtained. The Hamiltonian and overlap matrices **H** and **S** are expressed as

$$H_{L'S',LS} = \langle\Phi(k,L',s')|H_{a}|\Phi(k,L,s)\rangle \equiv \langle\Phi\,|H^{SR}|\Phi\rangle\,\delta_{s's} + \langle\Phi|H_{so}|\Phi\rangle \tag{10}$$

and

$$S_{L'S',LS} = S_{L'L}^{SR}\delta_{S'S} = [\mathbf{\Pi}^{+}\mathbf{\Pi} + \mathbf{\Omega}^{+}\langle\dot{\varphi}(L'',s)|\dot{\varphi}(L'',s)\rangle\mathbf{\Omega}]\delta_{S'S} \tag{11}$$

where

$$\langle\Phi|H^{SR}|\Phi\rangle = \mathbf{\Pi}^{+}\varepsilon_{l''s}\mathbf{\Pi} + \mathbf{\Pi}^{+}\mathbf{\Omega} + \mathbf{\Omega}^{+}\varepsilon_{l''s}\langle\dot{\varphi}(L'',s)|\dot{\varphi}(L'',s)\rangle\mathbf{\Omega} \tag{12}$$

$$\langle\Phi|H_{so}|\Phi\rangle = \mathbf{\Pi}^{+}\xi\Sigma\mathbf{\Pi} + \mathbf{\Pi}^{+}\dot{\xi}\Sigma\mathbf{\Omega} + \mathbf{\Omega}^{+}\dot{\xi}\Sigma\mathbf{\Pi} + \mathbf{\Omega}^{+}\ddot{\xi}\Sigma\mathbf{\Omega} \tag{13}$$

$$\xi\Sigma \equiv \langle\varphi(l'',m_{1},s')|H_{so}^{0}|\varphi(l'',m_{2},s)\rangle \tag{14}$$

$$\dot{\xi}\Sigma \equiv \langle\dot{\varphi}(l'',m_{1},s')|H_{so}^{0}|\varphi(l'',m_{2},s)\rangle \tag{15}$$

$$\ddot{\xi}\Sigma \equiv \langle\dot{\varphi}(l'',m_{1},s')|H_{so}^{1}|\dot{\varphi}(l'',m_{2},s)\rangle \tag{16}$$

where $\mathbf{H}^{SR}$ and $\mathbf{S}^{SR}$ denote the semi-relativistic representations of the Hamiltonian and overlap matrices. Matrix indices are omitted in the above equations.

Now the spin–orbit interaction is included in the total Hamiltonian and thus it can be treated simultaneously with the spin polarization in the self-consistent iteration procedure. The inclusion of spin–orbit interaction doubles the size of the **H** and **S** matrices in the secular equation because **H** and **S** are no longer block diagonal in spin components. The spin-up potential is used for the upper diagonal block and the spin-down potential for the lower diagonal block, whereas an averaged potential of the two is used for the off-diagonal block in calculating the above matrix elements. In fact, Daalderop *et al* [7] found that it does not make any significant difference whether one uses the spin-up or spin-down potentials or their average in constructing the matrix elements. We can solve the LMTO eigenvalue equation (9) by a standard diagonalization numerical technique to get the eigenvalues $\varepsilon_{j}(k)$ and the eigenvectors $C_{j}(k, L, s)$ at any given k-vector.

Hence

$$|\Psi_j(\boldsymbol{k})\rangle = \sum_{Ls} C_j(\boldsymbol{k}, L, s)|\Phi(\boldsymbol{k}, L, s)\rangle$$

$$\equiv \sum_{Ls} [A_j(\boldsymbol{k}, L, s)|\varphi(L, s)\rangle + B_j(\boldsymbol{k}, L, s)|\dot{\varphi}(L, s)\rangle]. \tag{17}$$

Here A and B are defined by multiplications of $\mathbf{C\Pi}$ and $\mathbf{C\Omega}$, respectively. From this, we can obtain the angular momentum-projected density of states (DOS):

$$N(\varepsilon) = \sum_{kj} \delta(\varepsilon - \varepsilon_j(\boldsymbol{k})) = \sum_{kj} \delta(\varepsilon - \varepsilon_j(\boldsymbol{k}))\, \langle \Psi_j(\boldsymbol{k}) \,|\Psi_j(\boldsymbol{k})\rangle$$

$$= \sum_{kj} \delta(\varepsilon - \varepsilon_j(\boldsymbol{k})) \sum_{Ls} [|A_j(\boldsymbol{k}, L, s)|^2 + |B_j(\boldsymbol{k}, L, s)|^2\, \langle \dot{\varphi}(L, s)\,|\dot{\varphi}(L, s)\rangle]$$

$$\equiv \sum_{Ls} N_{Ls}(\varepsilon) \tag{18}$$

where

$$N_{Ls}(\varepsilon) = \sum_{kj} \delta(\varepsilon - \varepsilon_j(\boldsymbol{k}))\, [|A_j(\boldsymbol{k}, L, s)|^2 + |B_j(\boldsymbol{k}, L, s)|^2\, \langle \dot{\varphi}(L, s)\,|\dot{\varphi}(L, s)\rangle]. \tag{19}$$

Spin and orbital magnetic moments are now derived as follows:

$$M_{\mathrm{sp}} = 2 \sum_{lms} s \int^{E_{\mathrm{F}}} N_{lms}(\varepsilon)\, \mathrm{d}\varepsilon \tag{20}$$

$$M_{\mathrm{orb}} = \sum_{lms} m \int^{E_{\mathrm{F}}} N_{lms}(\varepsilon)\, \mathrm{d}\varepsilon. \tag{21}$$

The von Barth–Hedin [15] interpolation formula is used for the exchange–correlation potential and the tetrahedron scheme for the Brillouin zone integrations is utilized. Band-structure calculations are performed over 80 $\boldsymbol{k}$-points in the irreducible Brillouin zone.

3. Results and discussions

3.1. Transition metal

In the case when 3d transition-metal-free ions are in an insulating solid, it is well known that the crystal-field splitting, which is much larger than the spin–orbit coupling, quenches the orbital angular momentum. In other words, the mean value of the angular momentum and the associated orbital magnetic moment vanish. Hence the existence of the orbital magnetic moment reflects a measure of the spin–orbit interaction effect.

We have investigated orbital polarizations in the magnetic transition metals Fe, Co and Ni, stemming from the spin–orbit interaction. Spin-polarized calculations with and without the spin–orbit interaction considered are performed on BCC and FCC Fe, HCP Co and FCC Ni. The BCC Fe is called the α-phase of iron which is the ground state and ferromagnetic. The FCC Fe is called γ-Fe which is a high-temperature phase and antiferromagnetic. Both HCP Co and FCC Ni are ground-state phases and ferromagnetic.

Crystalline magnetic anisotropy caused by the coupling of the direction of the spin magnetic moment and the orbital magnetic moment reduces the symmetry of the system.

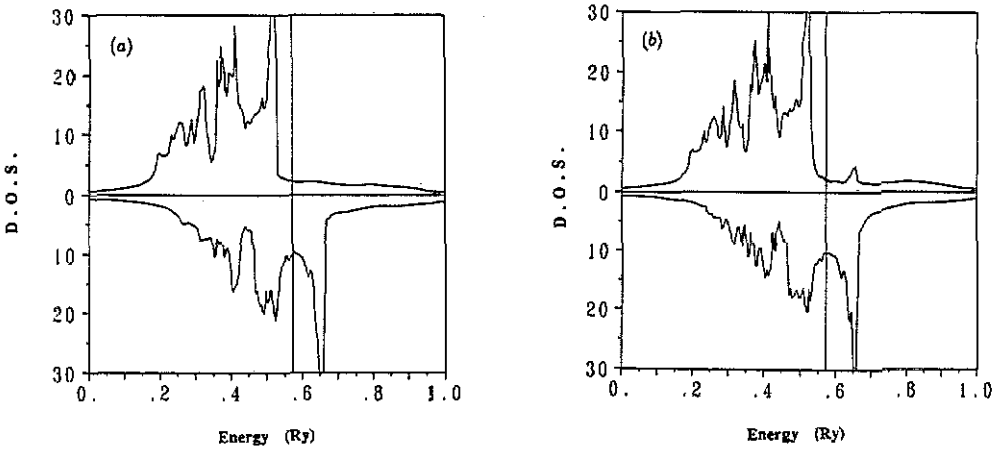

Figure 2. Spin-polarized DOS of HCP Co (*a*) without and (*b*) with the spin–orbit interaction included. The upper parts of the figures correspond to the spin-up band, and the lower parts correspond to the spin-down band.

The reduction in the symmetry gives rise to the anisotropy in the band structure along the formerly equivalent symmetry directions in the Brillouin zone. Implication from the detailed study by Daalderop *et al* [7], however, is that the effects of the symmetry reduction and the associated band-structure anisotropy on the magnitude of spin or orbital polarization are minor, although they can be crucial for the determination of the electronic properties near the Fermi level, such as the Fermi surface geometry. Hence, in the present study, we have not assumed any specific spin direction and kept the original crystal symmetry of the system in the band structure calculations with the spin–orbit interaction included.

Figure 2 displays the DOS of HCP Co which are calculated both with and without the spin–orbit interaction included. The overall shape of DOS calculated with the spin–orbit interaction is essentially identical with the semi-relativistic counterparts except for more split features seen in the states which is mostly d band-like. The DOSs at E_F are 12.3 states Ryd^{-1} and 12.6 states Ryd^{-1} for the cases with and without the spin–orbit interaction, respectively. The split features are due to hybridizations between spin-up and spin-down bands which remove most of the band intersections. Both calculations yield almost the same values of the spin magnetic moment, $1.62\mu_B$. The orbital magnetic moment mostly coming from the 3d-band orbital polarization is estimated to be $0.10\mu_B$.

The orbital contributions to magnetic moment for other materials are provided in table 1. Band-structure calculations are performed near the experimental lattice constants, $R_{WS} = 2.65$ for Fe, $R_{WS} = 2.62$ for Co and $R_{WS} = 2.60$ for Ni (R_{WS} is the Wigner–Seitz sphere radius). Note that the orbital magnetic moments are small, which are less than 10% of spin magnetic moments, but not negligible in these metals. Our results for BCC Fe, Co and Ni are in a good agreement with the previous results [7, 13, 16]. The magnitude of the orbital magnetic moment in Co is estimated to be the largest. As the spin–orbit interaction is introduced, the spin polarization is slightly reduced in BCC and FCC Fe ($0.01\mu_B$) while it slightly increases in Co ($0.01\mu_B$) and Ni ($0.03\mu_B$). The magnitude of the orbital magnetic moment in antiferromagnetic FCC Fe is twice that in ferromagnetic BCC Fe (0.06 versus 0.03). The spin magnetic moment and the exchange

Table 1. Calculated spin magnetic moments M_{sp} and orbital magnetic moments M_{orb} and the spectroscopic splitting g-factors for Fe, Co and Ni together with the previous results and experimental values: g^1, Our calculated value; g^2, value from [12]; g^3, value from [17]; g^4, value from [4]; g^5, value from [7]; g^6(exp), experimental value from [18].

	M_{sp} (μ_B)	M_{orb} (μ_B)	g^1	g^2	g^3	g^4	g^5	g^6(exp)
α-Fe	2.21	0.03	2.03	2.03	2.05		2.04	2.091
γ-Fe	1.72	0.06	2.07					
Co	1.62	0.10	2.12				2.11	2.187
Ni	0.63	0.06	2.19	2.17	2.14	2.15	2.17	2.183

Table 2. Spin magnetic moments M_{sp} and orbital magnetic moments M_{orb} for the ferromagnetic (F) and antiferromagnetic (AF) phases of BCC and FCC Fe.

		M_{sp} (μ_B)	M_{orb} (μ_B)
BCC Fe	F (α-Fe)	2.21	0.03
	AF	1.75	0.05
FCC Fe	F	2.41	0.08
	AF (γ-Fe)	1.72	0.06

splitting of the 3d band in antiferromagnetic Fe become reduced from those in ferromagnetic Fe. Generally the spin-up band yields a negative contribution to the orbital magnetic moment whereas the spin-down band yields a positive contribution [13]. Hence the effective shift of the Fermi level due to the reduced exchange splitting induces a change in the orbital magnetic moment, which is balanced between the positive and negative contributions from the partially filled spin-down band and the almost filled spin-up band, respectively. The real situation strongly depends on the detailed band structure of the system. Table 2, which provides the spin and orbital magnetic moments for both ferromagnetic and antiferromagnetic phases of BCC and FCC Fe, indicates that there is no simple correlation between the magnitudes of the spin and orbital magnetic moment. For FCC Fe the ferromagnetic phase has an even larger orbital magnetic moment than the antiferromagnetic phase, although the spin magnetic moment of the ferromagnetic phase is larger. The real shapes of the band structure and the DOS, which depend on both the crystal structure and the magnetic phase, are crucial factors for the size of the orbital magnetic moment.

With spin and orbital magnetic moments, the g-factor can be determined. There are two kinds of g-factor: the spectroscopic splitting factor g and the magnetomechanical ratio g'. The spectroscopic splitting g-factor is given by the ratio of the total magnetic moment to the spin angular momentum and the magnetomechanical ratio g' is given by the ratio of the total magnetic moment to the total angular momentum. The magnetomechanical ratio g' is related to the Landé g-factor of free ions with a partially filled shell. If we consider the components of the vector quantities in the direction of the magnetization (z direction), they are expressed as [17, 18]

$$g = (2m/e)(\langle M_z\rangle/\langle S_z\rangle) = 2(M_{sp} + M_{orb})/M_{sp} \tag{22}$$

$$g' = (2m/e)(\langle M_z\rangle/\langle S_z + L_z\rangle) = 2(M_{sp} + M_{orb})/(M_{sp} + 2M_{orb}). \tag{23}$$

When the orbital magnetic moment is zero, both g-factors become 2 as expected. The spectroscopic splitting g-factor can be measured directly from the ferromagnetic magnetic resonance.

There have been quite a few attempts to calculate the g-factors. Among those, Singh *et al* [17] and Fritsche *et al* [12] computed g-factors for Fe and Ni using the tight-binding method and the linear rigorous cellular band method, respectively. More recently, Krutzen and Springelkamp [4] reported the g-factor for Ni using the spin-polarized relativistic ASW band method and Daalerop *et al* [7] reported g-factors for Fe, Co and Ni using the LMTO band method. The spectroscopic splitting g-factors that we obtained are also given in table 1. For comparison, previously reported results and experimental values are presented together. Our results are close to the previous data, especially to those of Daalerop *et al* [7]. The agreement between calculated and experimental values is good for Ni but somewhat poor for Fe and Co. Calculated values are about 3% less than the experimental values in the cases of Fe and Co.

3.2. Rare-earth metals

In order to investigate the systematic behaviour of f-orbital polarizations for an increasing number of f electrons, spin-polarized calculations with and without the spin–orbit interaction taken into account are performed on some rare-earth metals. We consider a series of rare-earth metals from Ce to Gd except for Pm which is radioactive and so no structural data are known. The f electrons in rare-earth metals are rather localized and thus caution is needed in applying the band theory to these partially filled f-shell materials.

α-Ce, which is the ground-state phase at normal pressure, has a FCC structure and behaves as an enhanced Pauli paramagnetism. With increasing temperature, FCC γ-Ce becomes more stable, with a larger lattice constant and a localized magnetic moment. Pr and Nd have a DHCP structure, Sm has a typical and complicated Sm-type structure and Eu has a simple BCC structure. These four elements have rather complicated magnetic structures [19]. The ground state Gd has a HCP structure and is ferromagnetic. In this study, FCC structures are assumed for Pr, Nd and Sm, and ferromagnetic structures are assumed for all. Band calculations are performed at the experimental lattice constant for Pr to Gd, and for Ce the lattice constant of the γ-phase is used.

Figure 3 provides values of the spin and orbital magnetic moments for rare-earth metals considered. Most of the orbital magnetic moments come from the orbital polarization of the 4f band, and the polarizations of the other bands are very small. It is found that the sign of the spin and orbital moments is opposite for most of them and so the g-factors are less than 2 except for Gd. This is consistent with Hund's third rule which applies to the free rare-earth ions with less than half-filled f shells. More interestingly, a large cancellation occurs between spin and orbital magnetic moments in the light lanthanides Ce, Pr and Nd. On the other hand, the orbital polarizations in Eu and Gd, both of which have a nearly half-filled f band, are much smaller than the spin polarizations. This feature in the 4f band is in contrast with the case of the 5f-band actinides. The orbital magnetic moment of Am, which has a configuration isoelectronic with Eu $5f^7 7s^2$, is rather large and is estimated to be $-1.12\mu_B$ with a spin magnetic moment of $6.50\mu_B$ [20]. The difference is attributed to the more delocalized nature of the 5f band. As the spin–orbit interaction is introduced, the DOS at E_F and the total

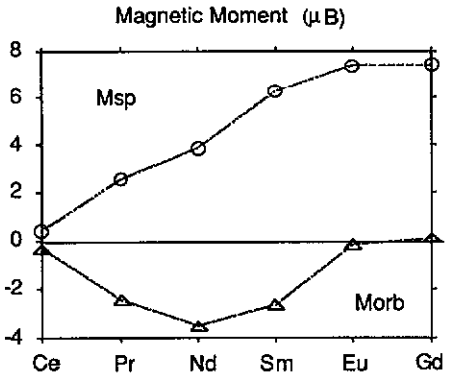

Figure 3. Spin magnetic moments M_{sp} (○) and orbital magnetic moments M_{orb} (△) of the rare-earth series.

energies decrease and spin polarizations are slightly reduced compared with the semi-relativistic values in most cases. Eu is an exception in that the spin polarization increases from $7.30\mu_B$ to $7.40\mu_B$ as the spin–orbit interaction is introduced.

Direct comparison of the calculated results with experiments is not appropriate because the real crystal structures and magnetic structures are different from those assumed in this study except for Gd. Furthermore, sufficient data for magnetic properties are not available for the light rare-earth metals owing to the difficult sample preparation and their inherent antiferromagnetic structures. As for Gd, our estimated values of the magnetic moment, $7.68\mu_B$ ($7.60\mu_B$ from the spin and $0.08\mu_B$ from the orbital magnetic moment), and the g-factor, 2.02 in Gd are close to the experimental values of $7.63\mu_B$ and 2.0 ± 0.02, respectively. A similar calculation for ferromagnetic Gd was reported by Sticht and Kübler [10] and Krutzen and Springelkamp [4]. The shape of the DOS obtained with the spin–orbit interaction included is essentially identical with their results. Different from other materials, the DOS at E_F increases as the spin–orbit interaction is introduced from 3.3 to 4.1 states eV^{-1}. Our value of the orbital magnetic moment, $0.08\mu_B$, is less than half the value of $0.25\mu_B$ obtained by Sticht and Kübler. We think that this discrepancy is attributed to the different exchange–correlation functionals and the different perturbation methods employed by Sticht and Kübler. On the other hand, our value is close to the value of $0.084\mu_B$ obtained by Krutzen and Springelkamp who used the same exchange–correlational functionals as ours (the von Barth–Hedin form). They reported that the spin and orbital magnetic moments are quite sensitive to the explicit form of the exchange–correlation functionals.

The behaviour seen in Eu and Gd metals, which possess rather small orbital polarizations, seems to be consistent with Hund's rule which applies to the free ions with a partially filled shell. The behaviour in light rare-earth metals, however, does not seem to follow Hund's rule. The magnitudes of the orbital moments are too small compared with the values of free ions anticipated from Hund's rule. Whether this fact is due to shortcomings of our approximation method or due to the different electronic structure between metals and free ions should be investigated further theoretically and also experimentally.

One always faces difficulties in dealing with the band structure of f-electron materials using the local-density approximation band calculations. This is due to the localized

nature of f electrons as well as to the subtle interplay between the spin polarization and the spin–orbit interaction. Jansen [21] argued that the orbital contribution is an important term in the total energy functionals. The orbital magnetic moment is caused by the spin–orbit interaction and also by the many-body correlation effects. He argued that the latter contribution is probably more important. Presumably, full relativistic spin-polarized band calculations with self-energy corrections which include the orbital moment contributions will provide a solution. An attempt has recently been made by Eriksson *et al* [22] to take into account the orbital moment correction in light lanthanides. Their suggestion is to incorporate Hund's second rule, which is not well treated in our perturbation method, to the evaluation of f-band eigenvalues using the Hartree–Fock theory. In this way, they have got much larger orbital polarizations for light lanthanides seemingly consistent with Hund's rule for free ions. This approach provides instructive directions towards the more general methods mentioned above; however, this is still an *ad hoc* approximation which adopts only the energy level shifts rather than the more accurate but unknown functional and the corresponding potential.

4. Summary

We have investigated the effects of the spin–orbit interaction on the electronic structures of magnetic materials—transition metals and rare-earth metals. A relativistic version of the LMTO band method is utilized which takes into account the spin–orbit interaction and the magnetic exchange–correlation interaction simultaneously.

For the transition metals Fe, Co and Ni, we have determined orbital polarizations and spectroscopic splitting g-factors both of which originate from the spin–orbit interaction. It is found that the 3d-band orbital magnetic moments in these materials are small but not negligible. The agreement between calculated and experimental values of g-factors is fairly good.

We have also studied the systematic behaviour of the orbital polarizations in light rare-earth metals as increasing the number of f electrons. It is found that in Ce, Pr and Nd the orbital magnetic moments nearly cancel the spin magnetic moments whereas in Eu and Gd the orbital magnetic moments are very small. The calculated values of the magnetic moment and the g-factor in Gd are in close agreement with experimental values.

Acknowledgments

This work was supported by the BSRI program (1990–1991) of the Korean Ministry of Education. Helpful discussions with A J Freeman, M R Norman, D D Koelling, T Oguchi and J-S Kang are greatly appreciated.

References

[1] Min B I, Jansen H J F, Oguchi T and Freeman A J 1986 *J. Magn. Magn. Mater.* **61** 139
[2] MacDonald A H and Vosko S H 1979 *J. Phys. C: Solid State Phys.* **12** 2977
MacDonald A H 1983 *J. Phys. C: Solid State Phys.* **16** 3869
Xu B, Rajagopal A K and Ramana M V 1984 *J. Phys. C: Solid State Phys.* **17** 1339, and references therein

Strange P, Staunton J and Gyorffy B L 1984 *J. Phys. C: Solid State Phys.* **17** 3355
Cortona P, Doniach S and Sommers C 1985 *Phys. Rev.* A **31** 2842
Eschrig H 1985 *Solid State Commun.* **56** 777
Schadler G, Weinberg P, Boring A H and Albers R C 1986 *Phys. Rev.* B **34** 2
Ebert H P 1988 *Phys. Rev.* B **38** 9390
[3] Ackermann B, Feder R and Tamura E 1984 *J. Phys. F: Met. Phys.* **14** L173
[4] Krutzen B C H and Springelkamp F 1989 *J. Phys.: Condens. Matter* **1** 8369
[5] Ebert H P, Strange P and Gyorffy B L 1988 *J. Phys. F: Met. Phys.* **18** L135
[6] Jansen H J F 1988 *Phys. Rev.* B **38** 8022
[7] Daalderop G H O, Kelly P J and Schuurmans M F H 1990 *Phys. Rev.* B **41** 11919
[8] MacDonald A H, Pickett W E and Koelling D D 1980 *J. Phys. C: Solid State Phys.* **13** 2675
[9] Brooks M S S and Kelly P J 1983 *Phys. Rev. Lett.* **51** 1708
[10] Sticht J and Kübler J 1985 *Solid State Commun.* **53** 529
[11] Norman M R and Koelling D D 1986 *Phys. Rev.* B **33** 3803
[12] Fritsche L, Noffke J and Eckardt H 1987 *J. Phys. F: Met. Phys.* **17** 943
[13] Eriksson O, Johansson B, Albers R C, Boring A M and Brooks M S S 1990 *Phys. Rev.* B **42** 2707
[14] Koelling D D and Harmon B H 1977 *J. Phys. C: Solid State Phys.* **10** 3107
[15] von Barth U and Hedin L 1972 *J. Phys. C: Solid State Phys.* **5** 1629
[16] Eriksson O, Nordstrom L, Pohn A, Severin L, Boring A M and Johansson B 1990 *Phys. Rev.* B **41** 11807
[17] Singh M, Callaway J and Wang C S 1976 *Phys. Rev.* B **14** 1214
[18] Wohlfarth E P (ed) 1980 *Ferromagnetic Materials* vol 1 (Amsterdam: North-Holland) p 35
[19] Gschneidner K A and Eyring L (ed) 1978 *Handbook on the Physics and Chemistry of Rare-earths* vol 1 (Amsterdam: North-Holland)
[20] Min B I 1990 unpublished
[21] Jansen H J F 1990 *J. Appl. Phys.* **67** 4555
[22] Eriksson O, Brooks M S S and Johansson B 1990 *Phys. Rev.* B **41** 7311